Surface-reconstruction-induced changes in free-carrier scattering from the W(100) surface: An infrared surface-electromagnetic-wave study

D. M. Riffe, L. M. Hanssen, and A. J. Sievers

Laboratory of Atomic and Solid State Physics and Materials Science Center, Cornell University, Ithaca, New York 14853-2501

(Received 10 February 1986)

Using the infrared-absorption technique of surface-electromagnetic-wave spectroscopy (SEWS) we have studied the effects of H_2 and D_2 chemisorption on the SEW attenuation coefficient α in the 10-μm region between 165 and 350 K. The change in α at room temperature has also been measured for N_2, O_2, and CO adsorption. The coverage (Θ) dependence of α for N_2, O_2, and CO is fairly simple [either a monotonic increase (N_2) or a peak at some intermediate coverage (O_2, CO)] and points to changes in free-carrier (FC) surface scattering as the dominant α-changing mechanism. Much richer structure in $\alpha(\Theta)$ upon H_2 and D_2 adsorption is observed: A small peak followed by a sharp dip at $\Theta=0.42$ monolayer (ML) ($\Theta=2$ monolayers $\equiv$ saturation), a broad maximum at $\Theta=1.28$ ML, and a value at $\Theta=2.0$ ML higher than for the clean surface. For $\Theta>0.42$ ML the variations are dominated by reconstruction-induced changes in FC scattering from the surface. The difference in α between $\Theta=1.28$ ML and saturation indicates that the $\Theta=1.28$ ML disordered surface phase and the $\Theta=2.0$ ML $p(1\times1)$-D phase are temperature independent between 165 and 300 K. Adsorbate-induced quenching of the W(100) 0.3-eV intrinsic surface states also contributes to the changes in α; the associated loss of oscillator strength is most apparent in a strong frequency dependence of α relative to the clean surface for D_2 adsorption. In addition, it is possible that a decrease in relaxation of the W(100) surface as Θ approaches 0.42 ML for H_2 or D_2 has some effect on the SEW attenuation by influencing the amount of FC interband scattering at the metal-vacuum interface.

I. INTRODUCTION

In 1952 Holstein[1] showed with a simple physical argument that the infrared (ir) absorptivity at a metal surface is larger if the conduction electrons colliding with the surface are diffusely rather than specularly reflected. The next year Dingle further developed the theory of the anomalous skin effect[2,3] from the formal equations of Reuter and Sondheimer[4] and applied his theory[5] to a large group of optical data which resulted in qualitative agreement as long as the electronic scattering from the surface was assumed diffuse. Other experimental results on the absorption of electromagnetic radiation[6-11] also indicate diffuse surface scattering. However, Bennett et al.,[12-14] using supersmooth substrates for ultrahigh vacuum (UHV) evaporated Au, Ag, and Al films measured in a dry N_2 atmosphere, were able to obtain ir reflection results which were consistent with specular scattering. Furthermore, by increasing the roughness of the substrate[14] they were able to increase the value of the diffuse scattering and thereby decrease the reflectivity. Their results suggest that a sample of sufficient quality can exhibit specular scattering.

Although the early prejudice was that only totally diffuse scattering was possible, in spite of a small amount of experimental evidence to the contrary,[15] many more recent experiments[16-22] show that specular scattering is possible for atomically smooth surfaces and that contamination due to chemisorption, which is necessarily present in all but careful UHV studies, need not inhibit all of the specular electronic reflection from the surface. The prob-

lem has been and continues to be to identify specularity in a quantitative manner. With the development of UHV surface probes has come the realization that surface reconstruction is a natural phenomenon which can be triggered in a variety of ways.[23] In this paper we describe our infrared investigation of free-carrier scattering at a metal surface as a function of adsorbate- and temperature-induced surface reconstruction.

The W(100)-H surface has been studied by a variety of UHV techniques which has enabled a fairly detailed structural picture to develop. In spite of the large quantity of data about this system no study has directly dealt with the interaction of the tungsten conduction electrons with the surface upon H_2 adsorption. Although optical absorption studies have been done on this system they have either concentrated on energies above 0.6 eV where interband transitions dominate the optical response,[24,25] or they have addressed only the question of the vibrational response of the adsorbate-adsorbent system.[26,27] Here we use the ir absorption technique of surface electromagnetic wave spectroscopy (SEWS) in the 125 meV (1000 cm^{-1}) region to study the surface scattering phenomenon.

We find that for H_2 and D_2 adsorption the largest contribution to the change in absorptivity in this energy range can be attributed to variations in the free-carrier scattering from the surface caused by adsorbate-induced surface reconstruction. In addition there is a contribution due to the quenching of intrinsic surface states (ISS) located near 0.3 eV which are inherent to this surface. In the next section we discuss background information on free-carrier contributions to the SEW attenuation coefficient with an

emphasis on the surface-assisted ir absorption process. In Sec. III the experimental details are presented. The results for the change in the SEW attenuation coefficient are described in Sec. IV: Room temperature (RT) exposure and coverage dependence for H_2 and D_2 is presented along with the frequency dependence and temperature dependence of D_2-induced variations. In addition, room temperature exposure results are presented for adsorption of N_2, O_2, and CO. In Sec. V we discuss these results and show that changes in the bulk Drude parameters in a small region (several lattice constants) near the surface are too small to account for the data. We then discuss the variations in attenuation in terms of the 0.3-eV ISS and the surface-assisted absorption process. The concluding section summarizes our results on electronic surface scattering from the W(100) surface.

II. FREE-CARRIER CONTRIBUTIONS TO THE SEW ATTENUATION COEFFICIENT

A. Drude model

The ability of any metal such as tungsten to absorb infrared radiation at room temperature depends upon the behavior of the conduction electrons within a skin depth δ (≈ 100 Å) of the surface. More specifically, in the Drude model, the conduction electron contribution α_{ce} to the SEW attenuation coefficient α for a metal-vacuum interface is related to the relaxation time τ of the charge carriers within δ by

$$\alpha_{ce} = \left[\frac{\omega}{\omega_p}\right]^2 \frac{1}{c\tau} \quad (\omega \ll \omega_p) ,$$

where ω is the frequency, ω_p the plasma frequency (both in rad/sec), and c the speed of light.[28] In the infrared near room temperature there are three contributions to $1/\tau$ which must be considered: the electron-electron scattering rate $1/\tau_{e-e}$, the electron-phonon scattering rate $1/\tau_\phi$, and an effective scattering rate due to collisions with the surface $1/\tau_s$. These processes are often treated as independent so that

$$\frac{1}{\tau} = \frac{1}{\tau_{e-e}} + \frac{1}{\tau_\phi} + \frac{1}{\tau_s} ;$$

hence, we first consider each one separately.

1. Electron-electron scattering

The electron-electron scattering rate has been theoretically considered by Gurzhi[29,30] and Lawrence.[31] Both authors have derived expressions for the scattering rate of the form

$$\frac{1}{\tau_{e-e}} = K\left[(k_B T)^2 + \left[\frac{\hbar\omega}{2\pi}\right]^2\right] .$$

Gurzhi's order-of-magnitude expression has $K \sim \omega_p / (\hbar\omega_p)^2$ which for tungsten is $\approx 2\times10^{14}$ s^{-1}eV^{-2}. [See Table I for ω_p (Ref. 32) and other ir parameters for W.] Lawrence's expression, which works fairly well for the noble metals Cu and Ag, yields values of $K \lesssim 10^{15}$ s^{-1}eV^{-2}.

TABLE I. Room-temperature ir parameters for W.

Parameter	Value at 1000 cm^{-1}
ρ_{dc}[a]	5.59 $\mu\Omega$ cm
$\hbar\omega_p$[b]	7.0 eV
v_F/c[c]	4.0×10^{-3}
v_F/ω	63 Å
δ[d]	140 Å
$1/\tau_{e-e}$[e]	1.4×10^{13} s^{-1}
$1/\tau_\phi$[f]	5.3×10^{13} s^{-1}
$1/\tau_s$[g]	$(1-p)1.6\times10^{13}$ s^{-1}
ϵ_0[h]	70

[a]Reference 41. [e]Reference 34.
[b]Reference 32. [f]See text.
[c]Reference 52. [g]Reference 1.
[d]Reference 50. [h]Reference 62.

Experimentally, the ω^2 and T^2 signatures allow $1/\tau_{e-e}$ to be determined from temperature-dependent emissivity measurements. For the transition metals Mo, V, Ta,[33] and W (Refs. 33 and 34) $1/\tau_{e-e}$ appears to be substantially larger than either of the theoretical estimations predict. In particular, for tungsten Wojcik et al.[34] have determined a value of $K = 1.4\times10^{16}$ s^{-1}eV^{-2}.[35] At room temperature and 1000 cm^{-1} this yields a value of $1/\tau_{e-e} = 1.4\times10^{13}$ s^{-1} which implies $\alpha_{e-e} = 0.15$ cm^{-1}.

2. Electron-phonon scattering

At zero frequency near room temperature electron-phonon scattering is the dominant relaxation mechanism for the free carriers and provides the major contribution to the dc resistivity $\rho_{dc} = 4\pi/[\omega_p^2\tau(0)]$.[36] For $\omega\neq0$ an extra decay mechanism exists due to the spontaneous emission of phonons which is absent in the zero-frequency limit.[37-39] This spontaneous emission process can produce a significant addition to the dc relaxation rate $1/\tau_\phi(0)$ for $\hbar\omega \gtrsim 2k_B T$ and $\hbar\omega \gtrsim 2k_B\Theta_D$ (Θ_D denotes the Debye temperature of metal).[39]

In the limits $\hbar\omega \gg k_B T$ and $\hbar\omega \gg k_B\Theta_D$ Holstein's[37,38] and Gurzhi's[39] results indicate at high temperatures ($T \gg \Theta_D$) that $1/\tau_\phi = 1/\tau_\phi(0)$. But as the temperature is lowered the spontaneous emission process gains increasing importance in the ir absorptivity until $T=0$, at which point it constitutes the only lattice vibrational decay mechanism of the electrons. For temperatures which are not too low ($T \gtrsim \Theta_D/4$) the relationship between the ir and dc relaxation rates is well represented by a second-order expansion in $(\Theta_D/T)^2$:

$$\frac{1}{\tau_\phi} = \frac{1}{\tau_\phi(0)}\left[1 + \frac{2}{18}\left[\frac{\Theta_D}{T}\right]^2 + \frac{11}{3240}\left[\frac{\Theta_D}{T}\right]^4\right] . \quad (1)$$

For tungsten $\Theta_D = 310$ K,[40] so a 12% correction to the dc rate results in the ir at room temperature.

Since $1/\tau_\phi(0)$ and $1/\tau_{e-e}(0)$ are the only significant RT contributions to ρ_{dc}, the electron-phonon relaxation rate can be calculated from ρ_{dc},[41] ω_p, $1/\tau_{e-e}(0)$,[42] and Eq. (1). Thus $1/\tau_\phi = 5.3\times10^{13}$ s^{-1} which implies $\alpha_\phi = 0.55$ cm$^{-1} \approx 3.7\alpha_{e-e}$ at 1000 cm^{-1}.

3. Electron-surface scattering

In the surface-assisted optical absorption process it is important to distinguish between scattering events which conserve the tangential velocity $v_{||}$ of the impinging electrons, which is defined as specular scattering, and those events which do not since $v_{||}$ conserving events contribute negligibly to the overall absorption.[1] The causes of nonspecular scattering can be conveniently divided into two categories.

The first category, which was considered by Holstein and Dingle, is composed of causes which are classified as surface disorder and leads to diffuse scattering. For a single crystal examples of such inhomogeneities are missing or extra atoms in the top layer, steps in the surface due to slight misalignment along a crystallographic axis, or, as is relevant to our discussion, adsorption of molecules onto the surface.

Nonspecular scattering also arises because of the complex nature of real Fermi surfaces and is present even in single crystals with perfect surfaces.[43–46] We refer to this process as surface umklapp scattering. To illustrate this for tungsten a slice of the Fermi surface,[47] normal to the (001) direction, is drawn in Fig. 1. It is composed of electron "jacks" and hole "octahedrals" and "ellipsoids." An electron located on the Fermi surface at point A will strike the (100) metal-vacuum interface at an incident angle of 45°. If the sample surface has the same periodicity as the lattice then the electron must be reflected to either
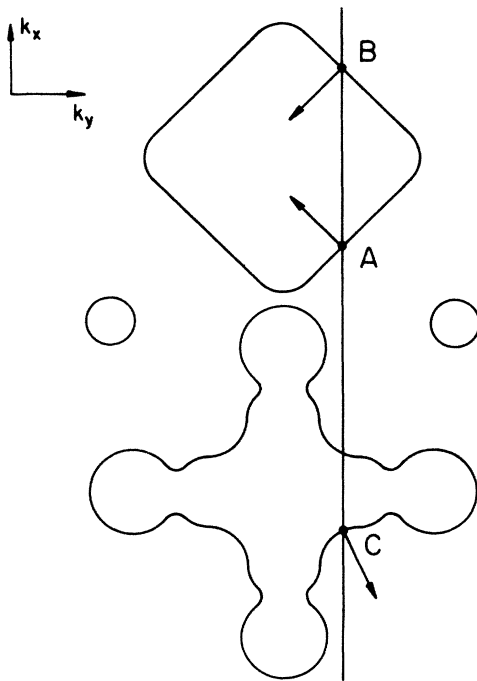
FIG. 2. α/α_ϕ versus frequency. The dashed lines show various contributions in the Drude model ($\alpha_\phi, \alpha_{e\text{-}e}$) with Holstein's approximation for diffuse surface scattering ($\alpha_{s,d}$). The solid lines are curves calculated from Dingle's anomalous skin effect equations.

FIG. 1. A slice of the W Fermi surface perpendicular to the (001) direction. An electron on the Fermi surface at point A (the vector indicates the direction of the electron's velocity) incident on the (100) metal-vacuum interface can be reflected to either point B or C with no change in tangential crystal momentum. Scattering into B is specular while scattering into C is a surface umklapp process.
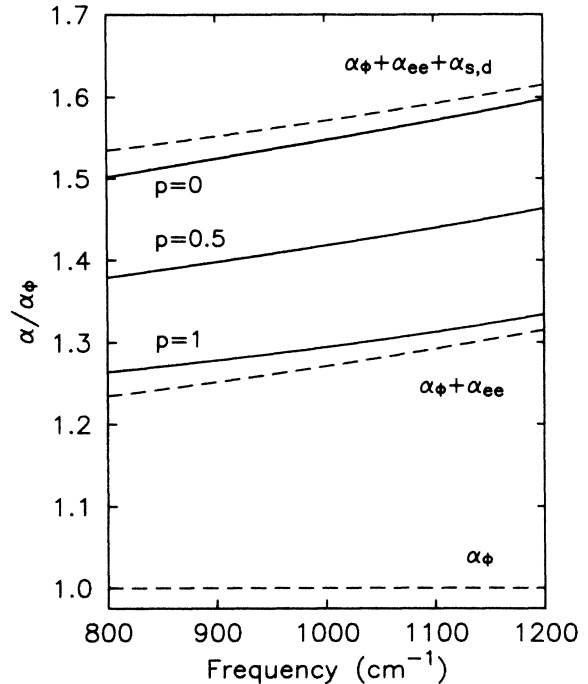
point B or C since the tangential crystal momentum $\hbar k_{||}$ is necessarily conserved. If it emerges in the state B then the scattering is specular since the tangential velocity is also conserved. Interband scattering from the free-carrier (FC) electron band to the FC hole band into the state C, however, results in a large change in the velocity parallel to the crystal surface, which contributes to ir absorption. An atomically perfect surface, therefore, need not appear perfectly specular.

The overall scattering behavior of conduction electrons from the surface is phenomenologically described by the Fuch's specularity parameter p.[48] If all the electrons are reflected with no tangential velocity change then $p=1$. $p=0$ indicates that the electrons are randomly scattered into all possible scattering angles. Other types of behavior can be characterized by a value of p between 0 and 1 which indicates the effective specularity of the outgoing electrons. For example, if all the electrons are reflected into angles near the specular direction then p is close to 1 even though there is no true specular scattering occurring.[49]

In order for the amount of specularity to have a major effect on the absorptivity of an optically thick sample two conditions must apply. The first is that the mean-free path l_0 of the electrons must be at least comparable to the classical skin depth δ (Ref. 50) of the metal. If $l_0 \ll \delta$ then bulk scattering dominates the absorptivity. The other condition is that the energy $\hbar\omega$ of the impinging radiation be below the region where interband transitions dominate the optical response of the metal. For good conduc-

tors at room temperature the range between 100 and 4000 cm^{-1} generally satisfies these two conditions,[51] below which $l_0 \ll \delta$ and above which interband transitions have the largest effect.

Within this range of frequencies there are two regions separated by $\delta = v_F/\omega$ (Ref. 52) (v_F is electronic velocity at Fermi surface). If the skin depth δ is much larger than the distance traveled by an electron in one cycle of the field then the dielectric function is local in space and the surface and bulk contributions can be separated.[1] In this case the surface contribution to the free-carrier response is characterized by a scattering rate

$$\frac{1}{\tau_s} = (1-p)\frac{3}{8}\frac{v_F}{c}\omega_p \ .$$

For tungsten this equals $(1-p)1.6 \times 10^{13}$ s^{-1} which implies $\alpha_s = (1-p)0.16$ cm^{-1} at 1000 cm^{-1}. In the diffuse limit $\alpha_{s,d} \approx 0.3\alpha_\phi$. In Fig. 2 α_ϕ, $\alpha_\phi + \alpha_{e\text{-}e}$, and $\alpha_\phi + \alpha_{e\text{-}e} + \alpha_{s,d}$ normalized by α_ϕ are plotted versus frequency.

B. Anomalous skin effect

Since for tungsten at 1000 cm^{-1}, $\delta \approx 2v_F/\omega$, Holstein's local description of the surface-assisted absorption process is not quite valid. Also, because SEW's are a p-polarized (TM) wave the effect on the absorptivity of microscopic fields located at the surface[53] must be considered along with the nonlocality of the dielectric function. Fortunately, as Kleiwer and Fuchs have shown,[54,55] for ω_p and τ appropriate for W near $\tilde{v} = 1000$ cm^{-1} the surface impedance $\hat{z}$ for non-normal incidence is independent of the polarization of the radiation and is essentially equivalent to that given by the theory of the anomalous skin effect as developed by Reuter and Sondheimer (RS).[4]

In the frequency region of interest Dingle[2,3] has calculated, using RS's equations, an expression for the surface impedance $\hat{z}$ which is appropriate for W at room temperature. Using the general relationship that $\alpha = -2(\omega/c)r_n x_n$ (Ref. 56) where r_n (x_n) is the real (imaginary) part of the normalized surface impedance $\hat{z}_n = \hat{z}/(4\pi/c)$ we have plotted, also in Fig. 2, α/α_ϕ for several values of p for the frequency region covered in our measurements. In the $\delta \gg v_F/\omega$ limit the results for $p=0$ and 1 approach the Drude-Holstein results for $(\alpha_\phi + \alpha_{e\text{-}e} + \alpha_{s,d})/\alpha_\phi$ and $(\alpha_\phi + \alpha_{e\text{-}e})/\alpha_\phi$, respectively.

III. EXPERIMENTAL

A. Sample details

The tungsten sample (6.1 cm $\times$ 0.6 cm $\times$ 0.17 cm) was oriented, spark cut, and then polished on both of its largest sides. Two gratings, used for coupling free-space radiation to the SEW's, were then etched into one of the polished surfaces with standard photolithographic techniques utilizing type J photoresist and a 5:1 mixture of HF and HNO$_3$ are the etchant. The 32-μm spacing gratings are an estimated 10 μm deep and are separated by 5 cm. The large distance between the gratings enhances the already high sensitivity SEWS affords over conventional reflec-

tion absorption spectroscopy when using a strong ir source such as a laser.[57]

The sample is mounted on a Huntington 600-XYZTRC manipulator in the UHV system and is thermally connected to a liquid-N$_2$ cooling assembly as shown in Fig. 3. Two feedthroughs on the manipulator flange are connected on the inside via a stainless-steel tube (f) through which liquid-N$_2$ flows. At the lowest point of the tube a copper block (h) is clamped onto it. Attached to the copper block two 0.025-cm-thick flexible, annealed copper strips (e) run down to the sample mount where they are sandwiched in place. The sandwich is necessary to electrically isolate the sample during cleaning or thermal desorption runs [since it is placed at high voltage via tantalum leads (l)] from the liquid-N$_2$ tube which is at ground. The sandwich consists of a stainless-steel block (j) which is connected to and held by the manipulator shaft (g), the copper cooling strips (e), a 1.9-cm-diam $\times$ 0.2-cm-thick sapphire flat (d), a 0.025-cm Ta sheet piece (c) indirectly connected to the sample, and a macor piece (i) for insulating the screws (k) which are
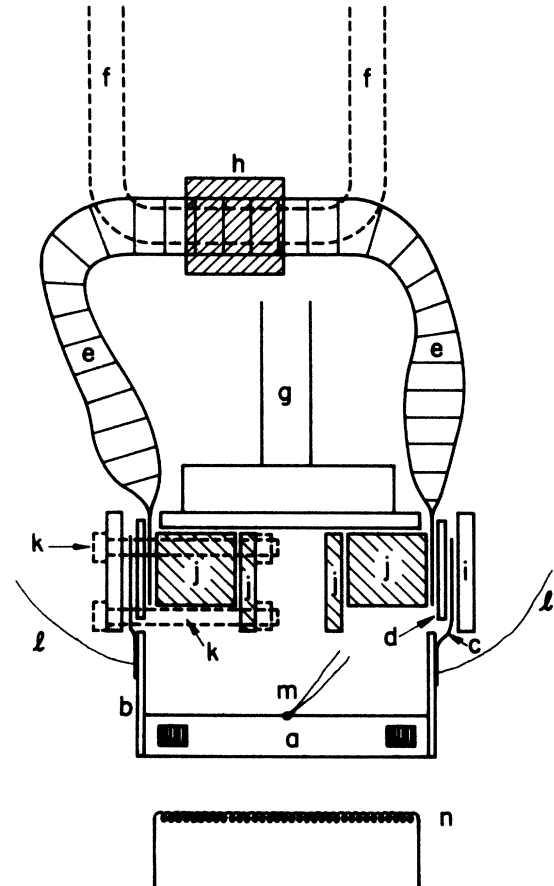

FIG. 3. A front sketch of the W sample mount. The sample (a) is thermally connected to the liquid-N$_2$ cooling feedthrough tube (f) via Ta rods (b), Ta sheets (c), sapphire flats (d), Cu sheet (e), and a Cu block (h). Macor pieces (i) and the sapphire flats electrically isolate the sample from ground during e-beam heating which is provided by the Ta filament (n) and the high-voltage Ta leads (l). Temperature is monitored with a W-Re(3 at. %)—W-Re(25 at. %) thermocouple (m).

used to squeeze the sandwich together (only shown dashed on left-hand side). The Ta strips are spotwelded to the Ta rods (b) which are electron-beam welded to the ends of the tungsten sample (a). By maintaining a constant flow of cold N_2 gas (or liquid) through the stainless-steel tube the sample cools from 2500 K to room temperature in 8 min and to 165 K in 25 min.

Sample temperature is measured with a W-Re(3 at. %)—W-Re(25 at. %) thermocouple (tc) (m) which is spotwelded to the center of the top edge of the sample. Above 298 K standard tables were used to determine the temperature, but below this the tc was calibrated against a Chromel-Alumel tc. This calibration differed by no more than ±2.0°C from the curve published by Sandstrom and Withrow.[58]

Before any measurements were made the sample was baked in 1×10^{-7} Torr of O_2 for about 20 h at 1520 K (with periodic flashes to 2300 K) via electron bombardment heating from a Ta filament (n) directly beneath the sample. After this treatment, the low-temperature $(\sqrt{2} \times \sqrt{2})R\,45°$ low-energy electron diffraction (LEED) pattern was observed, indicating that this procedure was sufficient to remove any C from the surface.[59] Before each experimental run the sample was again flashed to 2300 K to remove any contaminants, and the low-temperature LEED pattern was periodically observed as a check against subsequent C buildup.

B. Optical layout

The 32-μm spacing of the gratings was chosen so that the SEW's and free-space radiation couple near an angle of 45° at 1000 cm^{-1} as shown in Fig. 4. S-polarized (TE) radiation from a CO_2 laser (either $^{13}CO_2$ or $^{12}CO_2$) is sent through a chopper (C) and then a half-wave plate (WP) which is set to produce p-polarized (TM) radiation. (Because SEW's are a TM wave they only couple to TM free-space radiation.) Most of the radiation passes through a beam splitter (BS) and enters the vacuum chamber through a BaF_2 window ($W1$). A 40-cm focal length (FL) lens ($L2$) is used to focus the radiation onto the input grating where the SEW's are generated. The surface waves then travel the 5 cm across the W(100) surface to the output grating where they are converted back to free-space radiation which travels through another BaF_2 window ($W2$) and impinges on a liquid-N_2-cooled HgCdTe photoconductive detector ($D2$).

Although the free-space radiation generated at the output grating is well collimated its angle of departure changes as the frequency of radiation is changed. $L3$ is a 10-cm FL lens which images the output grating onto $D2$ and hence minimizes the need to realign the detector whenever the laser frequency is changed. The mirror ($M3$) mounted on a translation stage also minimizes problems in maximizing the detected signal whenever a new laser line is selected since translating $M3$ perpendicular to the axis of $L2$ changes the angle of incidence without altering the position of the incoming radiation on the sample.

The radiation which does not pass through the beam splitter is focused onto a pyroelectric detector ($D1$) by $L1$. The output signals of $D1$ and $D2$ are sent to separate
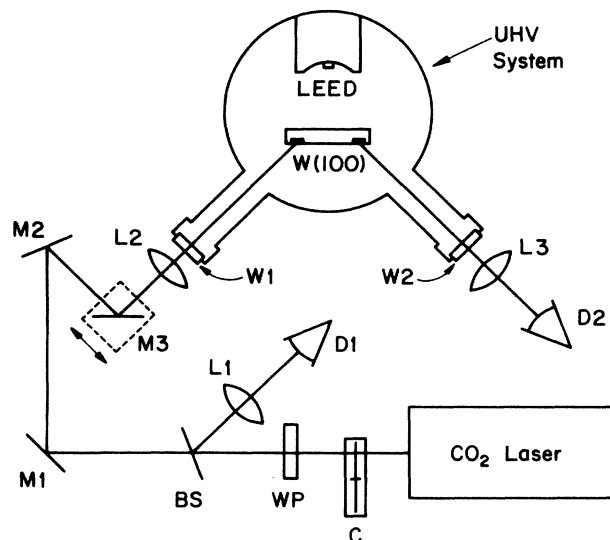

FIG. 4. Top view of the optical setup. A chopped CO_2 laser beam is sent into the sample chamber through a BaF_2 window ($W1$) and strikes the input grating of the sample. A HgCdTe detector ($D2$) is used to measure the transmitted intensity of free-space radiation generated at the output grating by SEW's which have traveled across 5 cm of the front (100) surface. LEED can be performed on the rear surface as ir measurements are made on the front. The ratio of the phase detected signals from $D2$ and the reference pyroelectric detector $D1$ are recorded on a chart recorder.

lock-ins tuned to the chopper frequency and their outputs are ratioed and recorded.

C. Experimental procedure

A typical experimental run consists of the following: The sample assembly is first cooled down as far as possible to insure as rapid cooling as possible from high temperatures. The sample is then flashed to 2300 K and allowed to cool to the desired adsorption temperature at which time the Ta filament is turned on and its current adjusted so that it radiatively stabilizes the sample temperature. Gas is then leaked into the chamber (typically at 5×10^{-9} Torr initially) and the SEW signal is monitored as a function of exposure. The change in the SEW attenuation coefficient α between two coverages Θ_i and Θ_f is calculated from $\Delta\alpha = -[1/(5 \text{ cm})]\ln(1+\Delta I/I_0)$ where ΔI is the change in the detected intensity I_0 between Θ_i and Θ_f.

IV. RESULTS

A. H_2 and D_2 adsorption

The features in $\Delta\alpha$ versus exposure are highly nonmonotonic and are qualitatively the same at all frequencies studied from 886 to 1088 cm^{-1}. Figure 5 shows two typical room-temperature runs, one for H_2 and one for D_2. Initial absorption results in a small, but significant, rise in α followed by a sharp minimum at an uncorrected gauge exposure of 0.100±0.004 (0.140±0.006) langmuir
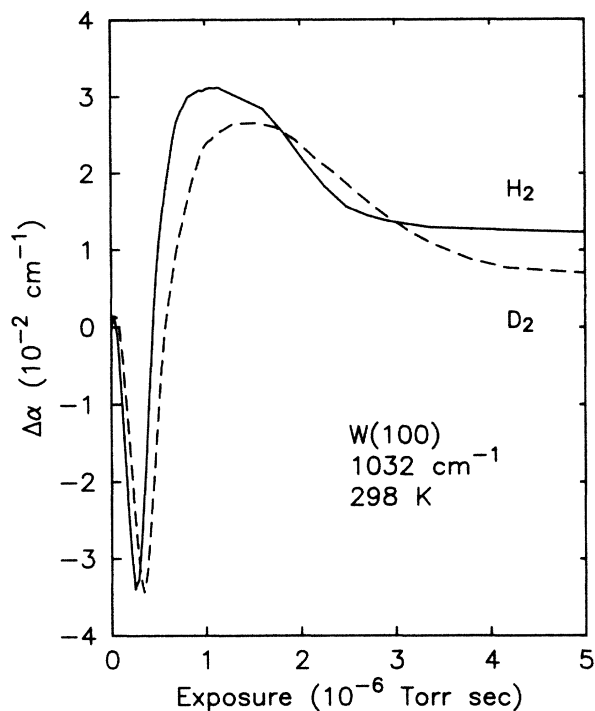
FIG. 5. Change in α versus exposure for H_2 and D_2 at a laser frequency of 1032 cm^{-1} and a temperature of 298 K. The exposure is a corrected value obtained by multiplying the ion gauge pressure by 2.3.
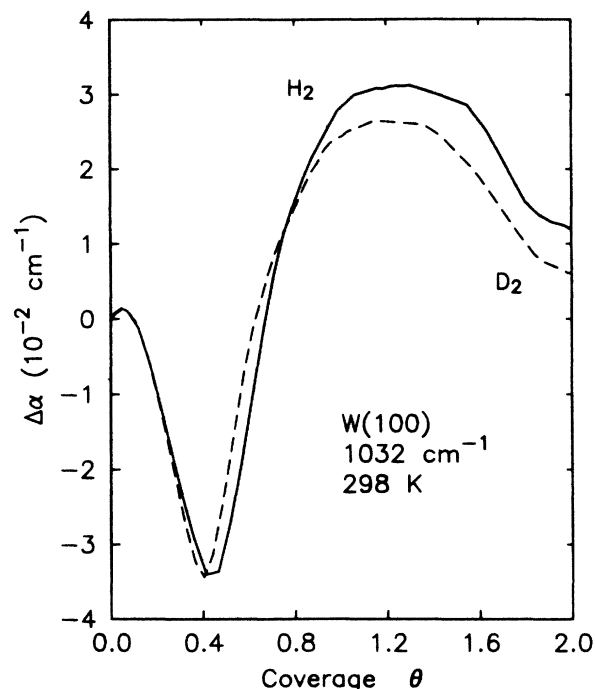

FIG. 6. Change in α versus coverage for H_2 and D_2 at a laser frequency of 1032 cm^{-1} and a temperature of 298 K. Coverage is determined from partial coverage thermal desorption measurements.

(L) for H_2 (D_2) (1 L$\equiv 10^{-6}$ Torr sec). This is followed by a rise to a broad maximum at 0.45±0.04 (0.59±0.05) L. (These exposure values are averages of all room-temperature runs.) As the surface becomes saturated α decreases to a final value above the zero coverage value with $\alpha_{H_2} > \alpha_{D_2}$. The stronger absorption for H_2 is mainly due to the W_2-H symmetric stretch (ν_1) which has been previously reported.[27] Note that the ratio of exposures at minimum α between D_2 and H_2 runs is 1.40±0.09, in good agreement with previous results that the sticking coefficient is the same for both isotopes.[60]

In order to convert exposure to coverage we use thermal desorption measurements which show that the coverage at the minimum is $\Theta = 0.42 \pm 0.04$ ML. Using this as a calibration point and the fact that the sticking coefficient is well represented by $s = C(1-\Theta/2)$ (Refs. 60 and 61) where C is a constant, the coverage for a given exposure is determined. $\Delta \alpha$ vs D_2 and H_2 coverage is shown in Fig. 6 for the same data shown in Fig. 5. The broad maximum now occurs at a coverage of $\Theta = 1.28 \pm 0.08$ ML.

Figure 7 shows the experimental results for $\Delta \alpha / \alpha_\phi$ for D_2 adsorption between various features (zero coverage, $\Theta = 0.42$ ML dip, $\Theta = 1.28$ ML peak and saturation) as a function of frequency. Data for D_2 instead of H_2 is presented in order to eliminate complications caused by the ν_1 mode absorption which is centered at 1070 cm^{-1} for the $p(1\times1)$-H state. Note that the data labeled B and C actually show a decrease in $|\Delta \alpha / \alpha_\phi|$ as ω increases while the data labeled A, D, and E show an increase.

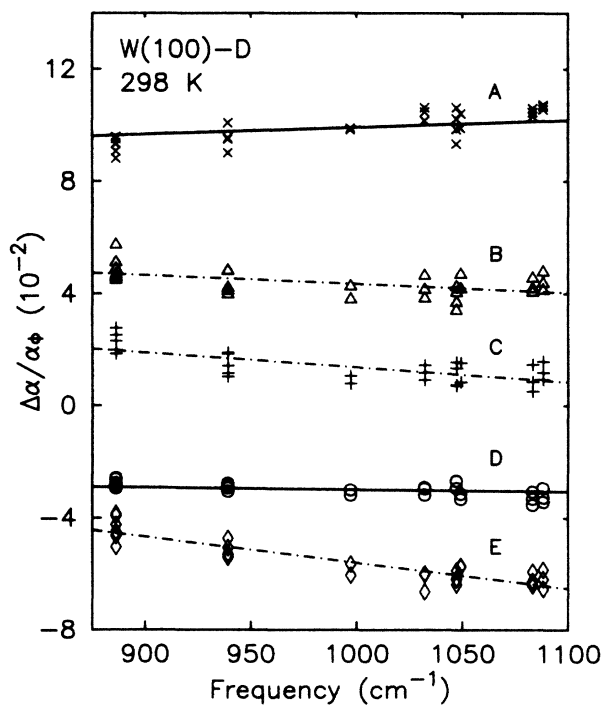The same basic features in $\Delta \alpha$ versus coverage for D_2

FIG. 7. Change in α versus frequency for D_2 adsorption between various initial (Θ_i) and final (Θ_f) coverages. Curve A, $\Theta_i = 0.42$ ML, $\Theta_f = 1.28$ ML; curve B, $\Theta_i = 0$ ML, $\Theta_f = 1.28$ ML; curve C, $\Theta_i = 0$ ML, $\Theta_f = 2.0$ ML; curve D, $\Theta_i = 1.28$ ML, $\Theta_f = 2.0$ ML; curve E, $\Theta_i = 0$ ML, $\Theta_f = 0.42$ ML. The solid lines are fits to the theory of the anomalous skin effect [Eq. (4)], while the dot-dashed lines are linear guides to the eye.
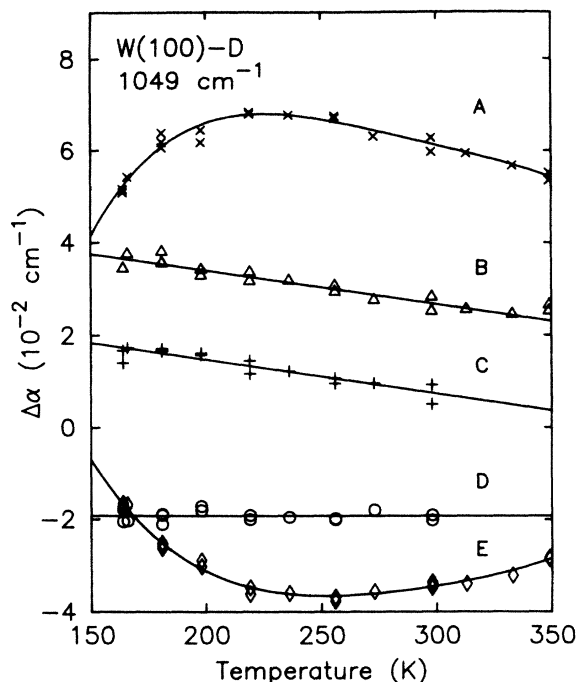
FIG. 8. Change in α between various coverages as a function of temperature. Curve A, $\Theta_i = 0.42$ ML, $\Theta_f = 1.28$ ML; curve B, $\Theta_i = 0$ ML, $\Theta_f = 1.28$ ML; curve C, $\Theta_i = 0$ ML, $\Theta_f = 2.0$ ML; curve D, $\Theta_i = 1.28$ ML, $\Theta_f = 2.0$ ML; curve E, $\Theta_i = 0$ ML, $\Theta_f = 0.42$ ML.
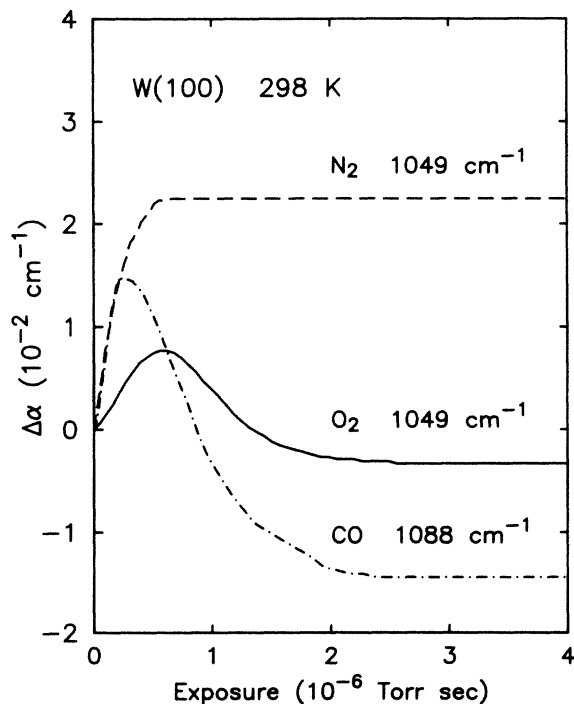

FIG. 9. $\Delta\alpha$ versus exposure for N_2, O_2, and CO at room temperature. The exposure is uncorrected in all cases.

and H_2 are present from 165 to 350 K. The temperature dependence of these changes for D_2 is shown in Fig. 8. We have drawn curves through the data labeled A and E as guides to the eye. The curves through B and C are linear fits below 300 K while a constant fit is shown for D. Above RT there is no data for $\Theta = 2.0$ ML since D_2 partially desorbs above 300 K.

B. Other gases

The rather complex nature of the coverage dependence of $\Delta\alpha$ for H_2 and D_2 prompted a look at the adsorption of other gases to see what similarities and differences might exist. Figure 9 shows RT results for adsorption of N_2, O_2, and CO onto the W(100) surface as a function of exposure. In each case the coverage dependence of the absorption is much simpler than for H_2 or D_2.

V. DISCUSSION

A. Changes in modified Drude parameters at the surface

Although tungsten is a transition metal, bulk ir data are well described by an appropriate plasma frequency ω_p, relaxation time τ, and high-frequency interband contribution ϵ_0 (Ref. 62) in a modified Drude model. One possible consequence of chemisorption is the alteration of these parameters in a small region (1 or 2 atomic layers) near the surface. Since the three-layer model of McIntyre and Aspnes[63] works well in interpreting the results of the W_2-H ν_1 mode absorption, we use it here to show that changes in the SEW attenuation coefficient α due to such effects are too small to account for the data.

For a sufficiently thin $(d/2\delta \ll 1)$ layer of thickness d, the attenuation due to the layer can be written as

$$\alpha_l = 8\pi^2 \tilde{v}^2 d \, \mathrm{Im} \left[\frac{1}{(-\hat{\epsilon}_m)^{1/2}} \left[\frac{\hat{\epsilon}_l - 1}{\hat{\epsilon}_l} + \frac{\hat{\epsilon}_l}{-\hat{\epsilon}_m} \right] \right] , \quad (2)$$

where ϵ_m (ϵ_l) is the dielectric function of the metal (layer) and $\tilde{v}$ is the frequency (cm^{-1}).[64] If we assume a modified Drude response

$$\hat{\epsilon}_k = \epsilon_{0,k} + i \left[\frac{\omega_{p,k}}{\omega} \right]^2 \frac{\omega \tau_k}{1 - i\omega\tau_k} \quad (3)$$

for the metal ($k = m$) and the layer ($k = l$), then the above effects correspond to altering $\omega_{p,l}$, τ_l, and $\epsilon_{0,l}$.

The change in α due to modifying the plasma frequency in a thin layer calculated from Eq. (2) and Eq. (3) is given by

$$\Delta\alpha = -\alpha_{ce} \frac{\Delta(\omega_{p,l}^2)}{\omega_{p,m}^2} \frac{d}{2\delta} .$$

Assuming that one conduction electron is tied up in each W—H bond this yields $\Delta\alpha = 1.5 \times 10^{-2} \Theta$ cm^{-1} at 1032 cm^{-1}. While this can account for the size of $\Delta\alpha$ at saturation it fails at lower coverages. Nor does it seem likely that the many variations in the sign of $\Delta\alpha$ as Θ in-

creases can be explained since all of the H is located at the bridge site[65] implying that the adsorbate-substrate bonding is basically the same at all coverages.

If instead $\epsilon_{0,l}$ is changed and $\omega_{p,l}^2$ is held at a fixed value on the order of $\omega_{p,m}^2$, then α is altered even less. In this case

$$\Delta\alpha = 3\alpha_{ce}\frac{\omega^2}{\omega_{p,m}^2}\Delta\epsilon_{0,l}\frac{d}{2\delta}$$

$$\approx 7\times 10^{-4}\Delta\epsilon_{0,l}\frac{d}{2\delta}\ \mathrm{cm}^{-1}\ .$$

Since $d/(2\delta)\approx 10^{-2}$ and the maximum in $\Delta\epsilon_{0,l}\approx 10^2$ (Ref. 66) we have result which is 2 orders of magnitude too small.

The largest excursion in α as the electron-phonon or electron-electron interaction is altered in a thin layer near the surface occurs as $\omega\tau_l$ increases from $\sim 7\times 10^{-2}$ to ~ 10 and results in $\Delta\alpha = 3\times 10^{-2}$ cm^{-1} for $d=3$ Å (≈ 2 atomic layers). While this is nearly large enough to be a possible explanation, more reasonable variations in τ_l, on the order of $\Delta\tau_l/\tau = 0.1$ cannot account for the size of the changes observed here. Hence it appears that changes in bulk parameters near the surface are insufficient to account for the SEWS observations.

B. Surface-assisted free carrier absorption: $\Theta > 0.42$ ML

The coverage region for $\Theta > 0.42$ ML shows best the free-carrier absorption effect for H$_2$ and D$_2$ adsorption. This is due to the fact that for $\Theta < 0.42$ ML the 0.3-eV intrinsic surface states are not yet quenched[67,68] and still contribute to optical absorption.[24] For this reason we first concentrate on $\Theta > 0.42$ ML.

Between $\Theta = 0.42$ and 2.0 ML the coverage dependence of the SEW attenuation coefficient (see Fig. 6) is similar to results for resistivity changes upon molecular adsorption onto thin metallic films.[69-71] In a number of these cases Wissmann[70] has demonstrated that the Fuchs theory of diffuse surface scattering[48] applies. The general features of the changes in resistivity upon chemisorption observed in these studies are as follows: Initial adsorption increases the diffuse scattering due to the randomness of adatom placement and leads to an initial increase in the resistivity. For some systems the diffuseness is a maximum at saturation, but for others there is a peak at some intermediate coverage(s). Such behavior is not unexpected since a saturated layer is often more uniform than one at intermediate coverages. A useful analogy is the Nordheim peak[72] in resistivity of a binary alloy A_xB_{1-x} as x is increased from zero to unity. In fact, a recent calculation including the effects of multiple scattering[73] has predicted the existence of such a maximum for an atomically smooth surface contaminated by adsorbed atoms. We also note a general experimental trend that the saturated coverage resistivity is consistently higher than the clean surface resistivity. The striking similarity between the W(100)-H (and -D) attenuation coefficient coverage dependence and the resistivity coverage dependence of thin gas covered films strongly points to changes in dif-

fuse surface scattering as the dominant mechanism for $\Theta > 0.42$ ML.

This interpretation is corroborated by other experimental results on this system. Figure 10 compares the SEW results with the mainly LEED-derived phase diagram[23,60,74,75] for the W(100)-H surface. (Henceforth we use H generically unless specifically referring to D.) At $\Theta = 0.42$ ML, where α is a minimum, the surface is reconstructed in what is known as the incommensurate—$c(2\times 2)$-H phase which is characterized by $\frac{1}{2}$ order spots split into a quartet along the $\pm(10)$ and $\pm(01)$ directions. As more gas is added the spots of the $\frac{1}{2}$ order quartet streak along directions perpendicular to their splitting (the streaking is apparent at $\Theta = 0.48$ ML for our sample) and then eventually disappear, indicating a loss of order in the one dimension followed by a loss of order in both dimensions. These LEED changes, signaling the onset of disorder, are accompanied by a sharp rise in the SEW attenuation until the maximum at $\Theta = 1.28$ ML. The subsequent fall in α as the surface approaches the well ordered $p(1\times 1)$-H state at saturation occurs concurrently with a decrease in the diffuse LEED background. The high degree of order at saturation is also reflected in high-energy ion scattering[76] results which show
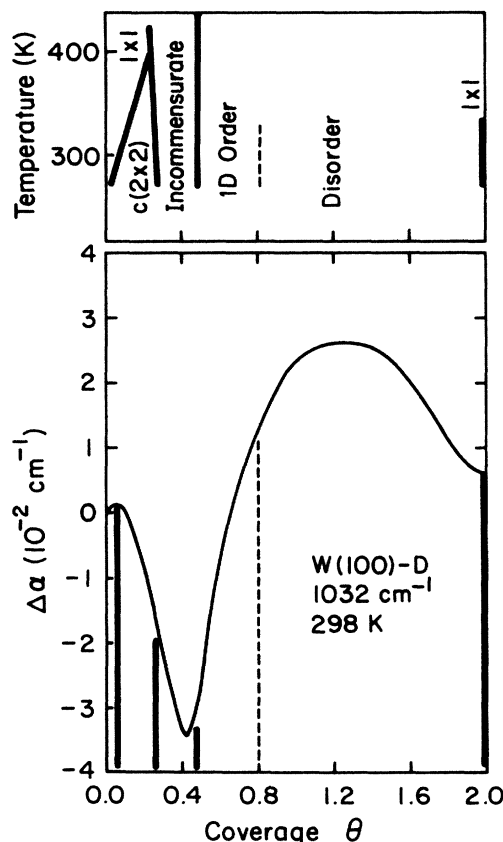

FIG. 10. The LEED determined phase diagram and $\Delta\alpha$ versus coverage for W(100)-D. The sharp dip occurs for the split—$c(2\times 2)$ phase while the broad maximum occurs for the disordered state. The boundaries on the incommensurate—$c(2\times 2)$ phase were determined from our LEED and thermal desorption measurements.

that the top layer is unreconstructed and in ir vibrational spectra which show that the v_1 and $2v_2$-β_1 absorption features are their sharpest at $\Theta = 2.0$ ML.[77]

The same basic coverage dependence also appears in the SEW data for the absorption of CO and O_2 as shown in Fig. 9: an initial rise in α followed by a peak at some intermediate coverage and a decrease towards saturation. Although the 0.3-eV ISS are quenched by adsorption of these gases, the quenching occurs more gradually;[67,68,78] hence the loss of the associated oscillator strength can be approximated by a slowly decreasing background. This appears to result in a smaller value of α at saturation compared with zero coverage. Nitrogen adsorption, on the other hand, shows no decrease in α after the initial rise, suggesting that disorder is a maximum at saturation for this system. These observations for the other gases further support the thesis that changes in diffuse surface scattering are being observed on the W(100) surface.

It should also be noticed that the variations in α for H_2 and D_2 are at least twice as large as for the other adsorbates. This seems strange since it is expected that the larger atoms should have a higher cross section for electronic scattering and suggests that it is the direct interaction of the free carriers with the reconstructed top W layer by H or D which results in the changes in α for these two systems.

In order to determine the amount the specularity changes we use the theory of the anomalous skin effect as developed by Dingle.[2,3] For the limited frequency range of our study Dingle's results can be summarized by the following equation:

$$\Delta\alpha/\alpha_\phi = -[0.253 + 6.3 \times 10^{-5}(\tilde{v} - 1000)]\Delta p , \qquad (4)$$

where $\tilde{v}$ is the frequency expressed in cm^{-1}. Using this equation we have determined the change in p between $\Theta_i = 0.42$ ML and $\Theta_f = 1.28$ ML to be $\Delta p = -0.39$ and between $\Theta_i = 1.28$ ML and $\Theta_f = 2.0$ ML to be $\Delta p = +0.11$. The fits are shown in Fig. 7 as the solid lines through the data labeled A and D. Although the frequency dependence of the data is slightly stronger than the theory, both show an increase in $|\Delta\alpha/\alpha_\phi|$ as ω increases.

The temperature dependence of the variations in α in this coverage range are interesting. The data labeled D in Fig. 8 shows that $\Delta\alpha$ between $\Theta_i = 1.28$ ML and $\Theta_f = 2.0$ ML is temperature independent from room temperature down to 165 K. This indicates that both of these phases are independent of temperature over this range, since it seems unlikely that the disordered and $p(1 \times 1)$-D states would change α in the same manner with temperature if there did exist a change in either one.

Using the value of α at $\Theta_f = 1.28$ ML as a reference the curve labeled A shows that as the temperature is lowered the relative attenuation at $\Theta_i = 0.42$ ML decreases until approximately 200 K where there begins a dramatic increase as the temperature is lowered further. The slow decrease suggests that the specularity for this phase increases slightly but that below 200 K it sharply drops off. Such a sharp drop in specularity may be associated with immobility of the adsorbate, as suggested by Barker et al.,[74] which hinders complete formation of the surface

phase. This immobility seems also apparent in other ir measurements where low-coverage, low-temperature modes are observed to be much broader than at room temperature.[79]

C. Surface umklapp scattering and the intrinsic surface states: $\Theta < 0.42$ ML

For $\Theta < 0.42$ ML it is apparent that something else besides surface assisted absorption contributes to the ir response. This is best seen in the frequency dependence of the changes in α for $\Theta_i = 0$ ML shown in curves B, C, and E of Fig. 7. For $\Theta_f = 1.28$ and 2.0 ML (curves B and C, respectively) $|\Delta\alpha/\alpha_\phi|$ shows a decrease as frequency increases while $|\Delta\alpha/\alpha_\phi|$ for $\Theta_f = 0.42$ ML (curve E) shows a much stronger dependence on frequency than curves A and D which show good agreement with the anomalous skin effect.

The resultant strong negative slope of $\Delta\alpha/\alpha_\phi$ versus frequency from these three $\Theta_i = 0$ ML curves can be understood in terms of the D_2 induced quenching of the 0.3-eV intrinsic surface states. As pointed out by Anderson et al.,[24] the good correlation of the surface reflectance spectroscopy (SRS) transition energies with the ultraviolet photoemission determined energy levels strongly suggests that the optical transitions from surface electronic states involve final-state energies located just above the Fermi level. Although the SRS measurements only probed transitions down to ≈ 0.6 eV the data show a contribution from these intrinsic states up to ≈ 0.8 eV, an indication that these states are rather broad. It is therefore reasonable to expect a contribution from the same states at 1000 cm^{-1} (0.125 eV). The strong frequency dependence is thus due to the fact that our measurements probe the low-frequency tail of these states where the absorption strength is rapidly changing.

Exactly how much these states contribute to the response is an open question and cannot be determined from this study. The simplest assumption is that all of the decrease in attenuation, after the small initial rise, is due to the quenching of optical transitions associated with the removal of the surface states. Another, perhaps more interesting, possibility is that some part of the large negative excursion in α is caused by the surface-enhanced free-carrier absorption effect. Although surface disorder is an unlikely explanation there is the possibility that surface umklapp processes play a role.

Surface disorder is largely ruled out by LEED observations in this coverage region.[23,60,74,75,80] The clean surface shows a mostly $p(1 \times 1)$ order (unreconstructed) with a hint of $\frac{1}{2}$ order spots. At a very small value of Θ the $\frac{1}{2}$ order spots sharpen considerably as the surface enters the $c(2 \times 2)$-H phase. With further coverage the $\frac{1}{2}$ order spots split into a quartet as described above as the incommensurate-$c(2 \times 2)$-H state is formed, with the magnitude of the splitting linearly proportional to the coverage beyond which the splitting begins to occur ($\Theta \approx 0.26$ ML for our sample). Although there is some debate about the state of the room-temperature clean surface (ordered versus disordered), both of the hydrogen stabilized phases definitely show long-range order.

At first glance one might assume that the appearance of $\frac{1}{2}$ order LEED spots would necessarily be associated with the opening up of more free-carrier nonspecular scattering channels. A look at Fig. 11, in which a slice of the Fermi surface[47] is drawn perpendicular to the (100) direction, indicates that this is not a large effect for W. A change in $k_{\parallel}$ corresponding to a $(\frac{1}{2} \frac{1}{2})$ LEED beam is drawn and shows for the majority of free carriers that such a change in parallel momentum is impossible since this momentum transfer connects relatively few states on the Fermi surface. Therefore, a $c(2\times2)$ structure should not significantly increase the diffuse surface scattering.

What may be occurring, though, is a change in the amount of surface umklapp scattering caused by adsorbate-induced changes in the relaxation of the W(100) surface. Since changes in reconstruction (periodicity parallel to this surface) can change the outgoing electrons' $k_{\parallel}$ it seems reasonable that a change in the first interatomic layer spacing (relaxation) could effect the outgoing $k_{\perp}$ and hence change the relative amount of electrons which are specularly reflected. Such a change in the relaxation of the first layer has been reported by King and Thomas[60] in their LEED study of this system. As Θ increases to ≈ 0.40 ML their Fig. 16 shows a sharp increase in the first W interlayer spacing of $\sim 2\%$, with much smaller subsequent variations as the surface becomes saturated.

The temperature dependence of $\Delta\alpha$ for the clean surface and a calculation by Fu et al.[81] lend mild support to this idea. Their calculation suggests that as the low-temperature $(\sqrt{2}\times\sqrt{2})R\,45°$ clean surface phase [which is quite similar to the $c(2\times2)$-H phase] is formed from the $p(1\times1)$ RT state the top layer spacing also increases (by $\sim 4\%$) to an unrelaxed position. A look at curves B and C of Fig. 8 shows that this phase transition is also accompanied by a decrease in the surface contribution to α, fur-

ther indicating that surface relaxation may be related to specularity through the surface umklapp mechanism.

Although the results of Fu et al. are consistent with a surface umklapp scattering explanation of the linear decrease in the clean surface contribution to α, another mechanism, related to the surface Debye temperature of W, may be responsible. The dynamical LEED data of Heilmann et al.[82] indicate that the high-temperature $p(1\times1)$ clean surface has an effective surface Debye temperature $\Theta_{D,S}=210\pm40$ K while the low-temperature $(\sqrt{2}\times\sqrt{2})R\,45°$ phase has an effective $\Theta_{D,S}=400\pm100$ K. Since in the temperature range of interest the electron-phonon relaxation rate $1/\tau_{\phi}\propto 1/\Theta_D^2$,[36] a change in $\Theta_{D,S}$ should effect the electron-phonon scattering in a thin layer near the surface. Using Eqs. (2) and (3) to estimate the change in α caused by the LEED determined increase in $\Theta_{D,S}$ yields $\Delta\alpha=-(8.0\pm3.0)\times10^{-3}$ cm^{-1} at 1049 cm^{-1} for a thickness equal to one interlayer spacing (1.6 Å). Experimentally, the change in α for the clean surface in going from 300 to 165 K is 1.0×10^{-2} cm^{-2}. The fact that the experimental and calculated values of $\Delta\alpha$ are not significantly different lends support to the idea that the change in $\Theta_{D,S}$ may be a possible explanation for the clean surface temperature dependence of $\Delta\alpha$.

Lastly, we note that initial adsorption results in a small, but perceptible, rise in α. It seems reasonable to suppose that this is due to an increase in diffuse surface scattering caused by a small increase in disorder of the surface due to random placement of the hydrogen before the $c(2\times2)$ order becomes long range.

VI. SUMMARY

We have investigated the behavior of changes in the attenuation coefficient of 10-μm SEW's caused by D_2 and H_2 adsorption on W(100). The variations have been discussed in terms of changing Drude parameters of the metal in a small region of the surface, the quenching of 0.3-eV intrinsic surface states, and surface-assisted free-carrier absorption. Changes in the Drude parameters of W in a thin layer near the surface are generally too small to account for the size of the observed variations.

For $\Theta>0.42$ ML there are four main experimental points which contribute to an interpretation that the variations in α are mainly the result of changes in the specularity of scattered free carriers caused by adsorbate-induced reconstruction of the W(100) surface atoms. The four points are as follows: (1) The maximum variation in α is quite large, i.e., it is 10 times larger than the W_2-H symmetric stretch contribution to α (Ref. 27) and at least 2 times larger than variations observed for CO, O_2, and N_2 adsorption. (2) A coverage dependence for α is observed which is similar to resistivity measurements on gas-covered films.[69-71] (3) There exists a high degree of correlation between the LEED deduced structures[60] and the variations. (4) The induced changes are broadband: they are observed over the entire range of frequencies studied from 886 to 1088 cm^{-1}, and they are fit well by the theory of the anomalous skin effect[2,3] with realistic values of changes in the Fuchs specularity parameter.[48]
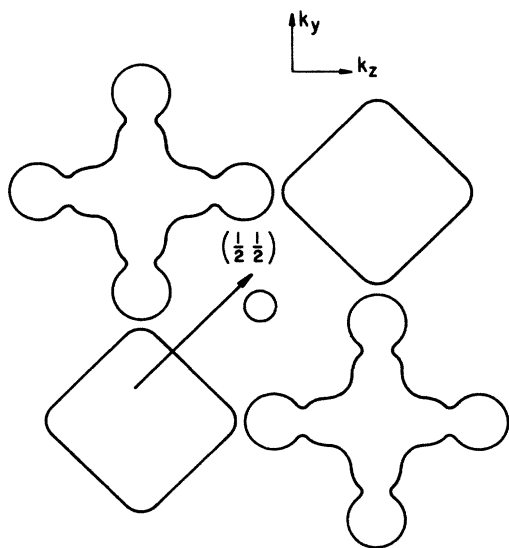
In this coverage range our results show that the

FIG. 11. A slice of the W Fermi surface perpendicular to the (100) direction, illustrating that a change in $k_{\parallel}$ corresponding to a $(\frac{1}{2} \frac{1}{2})$ LEED beam is forbidden for the majority of free carriers.

$\Theta = 1.28$ ML disordered surface phase and the saturation $p(1 \times 1)$-D phase are independent of temperature between 165 and 300 K. Also, the previously reported[74] immobility of the adsorbate below 200 K seems apparent for D_2 adsorption.

In the coverage range of $\Theta < 0.42$ ML it is shown that surface scattering is not the only mechanism for these broadband changes. Although the exact contribution of the 0.3-eV intrinsic surface states to the optical response at 10 μm is not known, it seems clear that they play some role. We suggest that surface umklapp scattering[43-46] may have some contribution to the large negative change

in α as Θ approaches 0.42 ML. In addition, the surface umklapp mechanism and/or a changing surface Debye temperature are possible explanations for the $\Theta = 0$ ML temperature dependence of $\Delta\alpha$.

ACKNOWLEDGMENTS

[1]T. Holstein, Phys. Rev. 88, 1427 (1952).

[2]R. B. Dingle, Physica 19, 311 (1953).

[3]R. B. Dingle, Physica 19, 729 (1953).

[4]G. E. H. Reuter and E. H. Sondheimer, Proc. R. Soc. London, Ser. A 195, 336 (1948).

[5]R. B. Dingle, Physica 19, 348 (1953).

[6]R. G. Chambers, Proc. R. Soc. London, Ser. A 215, 481 (1952).

[7]M. A. Biondi, Phys. Rev. 102, 964 (1956).

[8]E. W. Johnson and H. H. Johnson, J. Appl. Phys. 36, 1286 (1965).

[9]A. P. Lenham and D. M. Treherne, J. Opt. Soc. Am. 56, 683 (1966).

[10]M. A. Biondi and A. I. Guobadia, Phys. Rev. 166, 667 (1968).

[11]J. A. McKay and J. A. Rayne, Phys. Rev. B 13, 673 (1976).

[12]R. H. Doremus, J. Appl. Phys. 36, 2853 (1965).

[13]H. E. Bennett and J. M. Bennett, in Optical Properties and Electronic Structure of Metals and Alloys, edited by F. Abelès (North-Holland, Amsterdam, 1966), p. 175.

[14]H. E. Bennett, J. M. Bennett, E. J. Ashley, and R. J. Motyka, Phys. Rev. 165, 755 (1968).

[15]D. K. C. MacDonald and K. Sarginson, Proc. R. Soc. London, Ser. A 203, 223 (1950).

[16]E. J. Gillham, J. S. Preston, and B. E. Williams, Philos. Mag. 46, 1051 (1955).

[17]A. E. Ennos, Brit. J. Appl. Phys. 8, 113 (1957).

[18]M. S. P. Lucas, Appl. Phys. Lett. 4, 73 (1964).

[19]M. S. P. Lucas, Thin Solid Films 2, 337 (1968).

[20]D. C. Larson and B. T. Boiko, Appl. Phys. Lett. 5, 155 (1964).

[21]A. J. Learn and R. S. Spriggs, J. Appl. Phys. 34, 3012 (1963).

[22]K. L. Chopra, L. C. Bobb, and M. H. Francombe, J. Appl. Phys. 34, 1699 (1963).

[23]See, e.g., P. J. Estrup, in Chemistry and Physics of Solid Surfaces V, edited by R. Vanselow and R. Howe (Springer-Verlag, New York, 1984).

[24]J. Anderson, G. W. Rubloff, M. A. Passler, and P. J. Stiles, Phys. Rev. B 10, 2401 (1974).

[25]J. B. Restorff and H. D. Drew, Surf. Sci. 88, 399 (1979).

[26]Y. J. Chabal, Phys. Rev. Lett. 55, 845 (1985).

[27]D. M. Riffe, L. M. Hanssen, A. J. Sievers, Y. J. Chabal, and S. B. Christman, Surf. Sci. 161, L559 (1985).

[28]For a review of the properties of surface electromagnetic waves see, e.g., G. N. Zhizhin, M. A. Moskalova, E. V. Shomina, and V. A. Yakovlev, in Surface Polaritons, edited by V. M. Agranovich and D. L. Mills (North-Holland, New York, 1982), pp. 93–143.

[29]R. N. Gurzhi, Zh. Eksp. Teor. Fiz. 35, 965 (1958) [Sov. Phys.—JETP 8, 673 (1959)].

[30]R. N. Gurzhi, M. Y. Azbel, and H. P. Lin, Fiz. Tverd. Tela

(Leningrad) 5, 759 (1963) [Sov. Phys. Solid State 5, 554 (1963)].

[31]W. E. Lawrence, Phys. Rev. B 13, 5316 (1976).

[32]The value of $\hbar\omega_p$ in Table I was determined from an SEW interferrometric measurement on the sample used in this study; see L. M. Hanssen, Ph.D. Thesis, Cornell University, 1985; and L. M. Hanssen, D. M. Riffe, and A. J. Sievers (unpublished). A value of 6.0 eV has been obtained from the data of J. M. Weaver, C. G. Olson, and D. W. Lynch by M. A. Ordal et al., Appl. Opt. 22, 1099 (1983).

[33]S. X. Cheng and A. J. Sievers (unpublished).

[34]L. A. Wojcik, A. J. Sievers, G. W. Graham, and T. N. Rhodin, J. Opt. Soc. Am. 72, 149 (1982).

[35]This is essentially the same as the value determined by Cheng and Sievers in Ref. 33.

[36]F. J. Blatt, Physics of Electronic Conduction in Solids (McGraw-Hill, New York, 1968), pp. 183–196.

[37]T. Holstein, Phys. Rev. 96, 535 (1954).

[38]A brief derivation of Holstein's results is contained in the Appendix of Ref. 11.

[39]R. N. Gurzhi, Zh. Eksp. Teor. Fiz. 33, 660 (1957) [Sov. Phys.—JETP 6, 506 (1958)].

[40]N. W. Ashcroft and N. D. Mermin, Solid State Physics (Saunders College, Philadelphia, 1976), p. 461.

[41]C. J. Smithells, Tungsten (Chapman and Hall, London, 1952), p. 180.

[42]See previous section.

[43]P. J. Price, IBM J. Res. Dev. 4, 153 (1960).

[44]A. B. Pippard, The Dynamics of Conduction Electrons (Gordon and Breach, New York, 1965), pp. 46–51.

[45]R. F. Greene, in Solid State Surface Science (M. Dekker, New York, 1969), Vol. 1, pp. 87–132.

[46]A. F. Andreev, Usp. Fiz. Nauk 105, 113 (1971) [Sov. Phys.—Usp. 14, 609 (1972)].

[47]D. M. Sparlin and J. A. Marcus, Phys. Rev. 144, 484 (1966).

[48]K. Fuchs, Proc. Cambridge Philos. Soc. 34, 100 (1938).

[49]R. F. Greene, Phys. Rev. 141, 687 (1966).

[50]For tungsten at 10 μm $\delta \approx c / (2\omega_p)$.

[51]See, e.g., F. Wooten, Optical Properties of Solids (Academic, New York, 1972).

[52]The Fermi velocity is estimated from the ir plasma frequency assuming a spherical Fermi surface; see, e.g., N. W. Ashcroft and N. D. Mermin, Solid State Physics (Saunders College, Philadelphia, 1976), Chap. 2.

[53]P. J. Feibelman, Prog. Surf. Sci. 12, 287 (1982).

[54]K. L. Kliewer and R. Fuchs, Phys. Rev. 172, 607 (1968).

[55]J. M. Keller, R. Fuchs, and K. L. Kliewer, Phys. Rev. B 12, 2012 (1975).

[56]A. J. Sievers and Z. Schlesinger, J. Phys. (Paris) **44**, C10-13 (1983).

[57]Y. J. Chabal and A. J. Sievers, Phys. Rev. B **24**, 2921 (1981).

[58]D. R. Sandstrom and S. P. Withrow, J. Vac. Sci. Technol. **14**, 748 (1977).

[59]K. Yonehara and L. D. Schmidt, Surf. Sci. **25**, 238 (1971).

[60]D. A. King and G. Thomas, Surf. Sci. **92**, 201 (1980).

[61]T. E. Madey, Surf. Sci. **36**, 281 (1973).

[62]The value of ϵ_0 in Table I was obtained by L. V. Nomerovannaya, M. M. Kirillova, and M. M. Noskov, Zh. Eksp. Teor. Fiz. **60**, 748 (1971) [Sov. Phys.—JETP **33**, 405 (1971)] using ellipsometric techniques. A similar value can be obtained from the data of J. H. Weaver *et al.* in the paper by M. A. Ordal *et al.* (see Ref. 32).

[63]J. D. McIntyre and D. E. Aspnes, Surf. Sci. **24**, 417 (1971).

[64]Z. Schlesinger and A. J. Sievers, Phys. Rev. B **26**, 6444 (1982).

[65]M. R. Barnes and R. F. Willis, Phys. Rev. Lett. **41**, 1729 (1978).

[66]This value of $\Delta\epsilon_{0,l}$ is estimated from the value of $\epsilon_{0,m} = 70$ (see Ref. 62).

[67]B. J. Waclawski and E. W. Plummer, Phys. Rev. Lett. **29**, 783 (1972).

[68]B. Feuerbacher and B. Fitton, Phys. Rev. Lett. **29**, 786 (1972).

[69]J. W. Geus, in *Chemisorption and Reactions on Metallic Films*, edited by J. R. Anderson (Academic, New York, 1971), Vol.

1, p. 327, and references therein.

[70]P. Wissmann, in *Springer Tracts in Modern Physics*, edited by G. Höhler (Springer-Verlag, New York, 1975), Vol. 77, and references therein.

[71]C. Pariset and J. P. Chauvineau, Surf. Sci. **47**, 543 (1975).

[72]N. F. Mott and H. Jones, *The Theory of the Properties of Metals and Alloys* (Dover, New York, 1958), p. 297.

[73]D. Lessie, Phys. Rev. B **20**, 2491 (1979).

[74]R. A. Barker and P. J. Estrup, J. Chem. Phys. **74**, 1442 (1981).

[75]A. H. Smith, R. A. Barker, and P. J. Estrup, Surf. Sci. **136**, 327 (1984).

[76]I. Stensgaard, L. C. Feldman, and P. J. Silverman, Phys. Rev. Lett. **42**, 247 (1979).

[77]Y. J. Chabal, J. Electron Spectrosc. Relat. Phenom. **38**, 159 (1986).

[78]E. W. Plummer and J. W. Gadzuk, Phys. Rev. Lett. **25**, 1493 (1970).

[79]Y. J. Chabal (private communication).

[80]R. A. Barker and P. J. Estrup, Phys. Rev. Lett. **41**, 1307 (1978).

[81]C. L. Fu, A. J. Freeman, E. Wimmer, and M. Weinert, Phys. Rev. Lett. **54**, 2261 (1985).

[82]P. Heilmann, K. Heinz, and K. Müller, Surf. Sci. **89**, 84 (1979).